Hydrogen Fluoride Chemical Laser Amplifier Performance: Experiment

L. H. Sentman,* R. E. Waldo,† P. T. Theodoropoulos,† T. X. Nguyen,† and D. L. Carroll†
University of Illinois, Urbana, Illinois 61801

Performance data for a continuous-wave hydrogen fluoride (cw HF) chemical laser master oscillator/power amplifier showed that, regardless of the oscillator or resonator used to generate the input beam, the amplification ratio is an inverse function of the input power (intensity) and, for maximum amplification, the peak of the input intensity distribution must be matched to the peak of the zero power gain distribution in the amplifier. The match/mismatch of the oscillator/amplifier flowfields has a second-order effect on amplifier performance. The measured P_{out} vs P_{in} performance curve showed that, after a continuous increase, the difference $P_{out} - P_{in}$ remained almost constant over a wide range of input powers. These data showed that between one-third and one-half of the device's oscillator output must be input to obtain amplifier output equal to the device's oscillator performance. When the input beam contained time-dependent oscillations, the amplitude modulation of the output beam was reduced by a factor that equaled the amplification ratio of the amplifier.

Nomenclature

P_{in} = input power to the amplifier
P_{out} = output power from the amplifier
X_{ib} = distance of the optical axis of the input beam downstream from the H_2 injectors of the amplifier
Δ = $P_{out} - P_{in}$

I. Introduction

A REVIEW of the open literature on master oscillator/power amplifier configurations showed that there are very few data. The most extensive work was that done by UTRC.[1] However, due to the spectral mismatch between the oscillator and the amplifier, only $P_1(4)$ single-line amplification data for one location of the optical axis of the input beam were obtained. The experiments by Hoffman et al.[2] and Patterson et al.[3] were with pulsed HF and KrF systems, respectively. The recent cw HF amplifier work by Bernard et al.[4] used an optical trombone to constructively combine two amplified beams. The constructive beam combination was verified with a Michelson interferometer. The present experiments provide the first extensive data on cw HF amplifier performance as a function of input power, location of the optical axis of the input beam, flowfield match/mismatch between the oscillator and amplifier, flow rates in the amplifier, oscillator resonator type (stable or unstable), and the time-dependent oscillations of the input beam.

A Helios CL I laser (15 cm gain length) or a Helios CL II laser (30 cm gain length) was used as the oscillator while another Helios CL II laser was used as the amplifier. The CL IIs are identical, two-channel, arc-driven, subsonic, cw HF chemical lasers. The flow channel of the CL I laser is identical to one of the flow channels of the CL II lasers. This permits the flowfields of the oscillator and amplifier to be identical when the CL I laser is run at one-half the flow rates of the CL II laser. Section II presents the experimental zero power gain data for the amplifier. Section III contains experimental amplifier performance data. The effects of the resonator and time-dependent oscillations on amplifier performance are presented in Sec. IV. Section V contains concluding remarks.

II. Zero Power Gain Measurements

Zero power gain (ZPG) is the gain measured when the intensity of the probe beam is low enough that the probe beam does not perturb the media. This gain is often referred to as the small signal gain. Preliminary amplifier measurements[5] showed that the amplifier gain is inversely proportional to input power (intensity). An increase in input power results in an increase in input intensity, which in turn stimulates more radiation and begins to saturate the gain. As the input power decreases, the gain in the amplifier increases until at some point (P_{in} ZPG), it becomes equal to the zero power gain. Further decrease of the input power does not have any effect on the gain measured. This is the criterion for determining when the zero power gain region has been reached. A power less than or equal to P_{in} ZPG was used to measure zero power gain.

The CL I (operated single line for the zero power gain experiments and multiline for the amplifier experiments) was used as the oscillator. At the pressure and temperature of the flow in the gain zone of the CL I, the HF line width is about 400 MHz. With a mirror spacing of 1 m, there were only one or two longitudinal modes lasing. The CL II flow channel is 3.0 mm high and 355.6 mm wide with a clear aperture 3.0 mm high × 40.0 mm wide. A schematic of the experimental layout is shown in Fig. 1. The input beam from the CL I was reduced in size by a two-lens telescope (first lens 250 mm focal length CaF_2 plano-convex, second lens −50 mm focal length CaF_2 plano-concave) to eliminate clipping of the input beam by the amplifier flow channel. The optical axis of the input beam was centered on the location of the H_2 injectors and passed through the CL II parallel to the H_2 injectors (X_{ib} = 0). This locates the optical axis of the beam within the CL II amplifier gain medium so that the beam geometry in the amplifier gain medium is similar to the beam geometry in the oscillator gain medium. By moving the translation stage on which the injection optics (the #2 turning mirror and the telescope) were located, the axis of the input beam was moved downstream of the H_2 injectors to measure amplification as a function of the location of the axis of the input beam, X_{ib}.

The input power required to measure the zero power gain of each line was obtained by measuring the amplification ratio (AR = P_{out}/P_{in}) as a function of the input power at the point in the amplifier flowfield corresponding to maximum ampli-

Received July 16, 1990; revision received March 9, 1991; accepted for publication April 28, 1991. Copyright © 1991 by the American Institute of Aeronautics and Astronautics, Inc. All rights reserved.

*Professor, Aeronautical and Astronautical Engineering Department. Associate Fellow AIAA.

†Research Assistant, Aeronautical and Astronautical Engineering Department. Student Member AIAA.

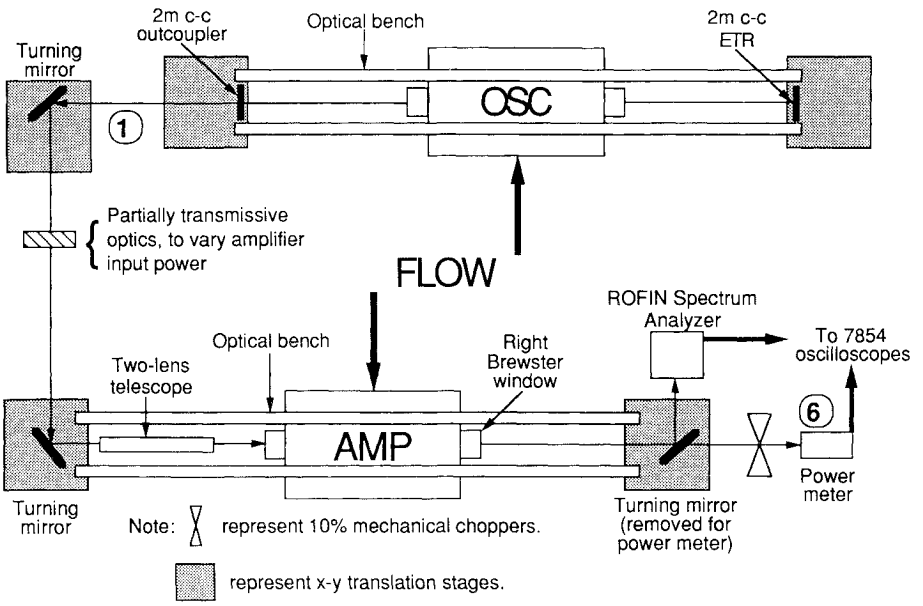

Fig. 1 Schematic of the experimental layout for zero power gain and amplifier performance studies.

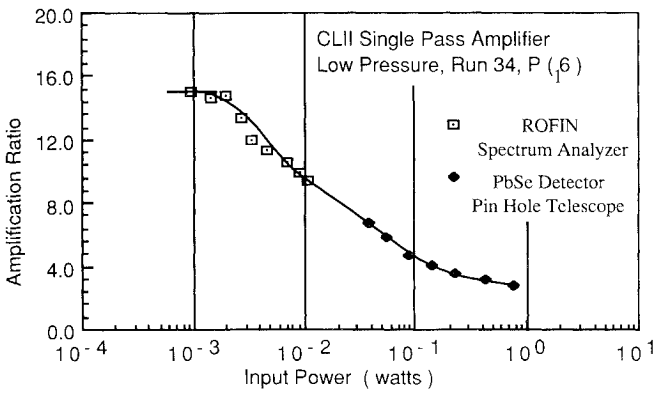

Fig. 2 Variation of amplification ratio with input power. The zero power gain region is reached when $P_{in} < 0.002$ W. Error bars smaller than the symbols are not shown.

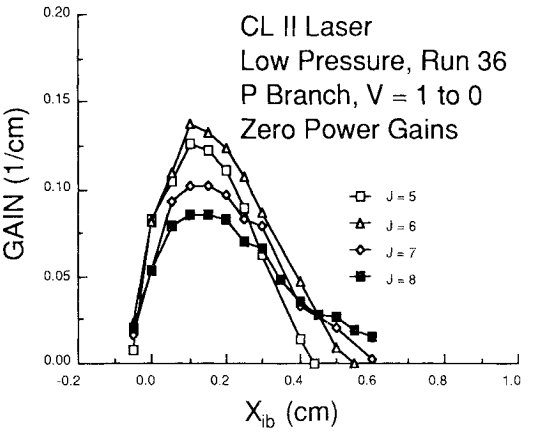

Fig. 3 Variation of the zero power gain as a function of distance downstream from the H_2 injectors for several $P_1(J)$ lines. The H_2 injectors are located at $X_{ib} = 0$. Error bars smaller than the symbols are not shown.

fication. When the AR became constant, independent of P_{in}, the zero power gain region had been reached (Fig. 2). Because of the low input powers required to reach the zero power gain region (of the order of 0.002 W), a ROFIN RSO 6000 Series Optical Spectrum Analyzer was used to measure the AR when the input power of the probe beam became too low for the PbSe detector to be accurate.[5]

The input power required to measure the ZPG of each line was established for two flow rates in the amplifier,[5] (Run 34: He = 0.0874, O_2 = 0.294, SF_6 = 0.71, and H_2 = 0.0356 g/s; Run 36: He = 0.0874, O_2 = 0.294, SF_6 = 1.07, and H_2 = 0.0514 g/s). The low-pressure ZPGs for each line as a function of X_{ib} were measured for both Run 34 (static pressure of 5.4 Torr 5.0 mm downstream of the H_2 injectors) and Run 36 (6.5 Torr) flow rates in the amplifier. The temperature and velocity of the flow in the gain zone are estimated from the computer model[6] as 450 K and 20,000 cm/s. Higher gains were measured at Run 36 flow rates than at Run 34 flow rates. At Run 36 flow rates, the lines with the highest gains are $P_1(5)$ and $P_1(6)$ for the 1→0 vibrational band and $P_2(5)$ and $P_2(6)$ for the 2→1 vibrational band (Figs. 3 and 4). The $P_2(J)$ peak ZPGs are about 1.46 times larger than the $P_1(J)$ peak ZPGs. The $P_1(J)$ gain zone is about 1.3 times longer than the $P_2(J)$ gain zone. The $P_1(J)$ ZPGs peak 1.5–2.0 mm downstream of the H_2 injectors, while the $P_2(J)$ ZPGs peak 1.0 mm downstream of the H_2 injectors.

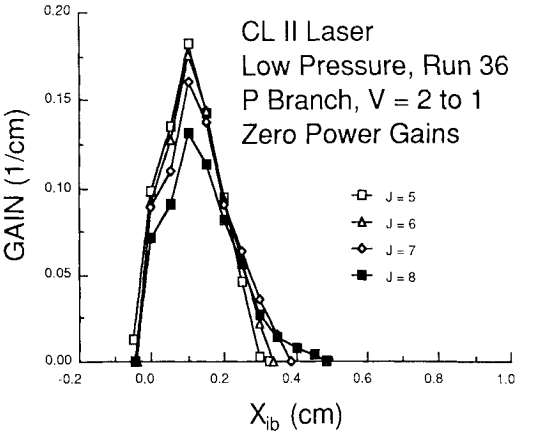

Fig. 4 Variation of the zero power gain as a function of distance downstream from the H_2 injectors for several $P_2(J)$ lines. The H_2 injectors are located at $X_{ib} = 0$. Error bars smaller than the symbols are not shown.

The effect of polarization on zero power gain was studied by comparing zero power gain data obtained with a vertically polarized, a horizontally polarized, and an unpolarized probe beam. These data showed that polarization does not affect zero power gain.[5]

The effect of high pressure on the ZPG was investigated for lines $P_1(6)$, $P_2(5)$, and $P_2(6)$[5] for the Run 34 flow rates at a cavity pressure of 10.0 Torr. The high-pressure ZPGs of these three lines were measured as a function of X_{ib} at the same input powers that were used to measure their low-pressure ZPGs. The high pressure (which increased the collisional deactivation rates) results in ZPG zones that are considerably shorter than those measured at low pressure. The peak ZPG of $P_1(6)$ was not affected by high pressure, but the peak ZPGs of $P_2(5)$ and $P_2(6)$ were decreased by about 22.5%. This is a result of the fact that the increased collisional deactivation of HF(2) repopulates HF(1), thereby keeping the population difference between HF(1) and HF(0) about the same, whereas the population difference between HF(2) and HF(1) decreased. High pressure caused the location of the peak ZPG to occur 0.5 mm closer to the H_2 injectors for all three lines.

III. Amplifier Performance

To determine the conditions under which an amplifier can be operated efficiently, the parameters that control amplifier performance must be identified. A previous study[5] showed that amplifier performance is a strong function of P_{in} to the amplifier where the amplifier performance parameters are AR and P_{out}. Both measures of amplifier performance are needed because each measure by itself results in a trivial situation, i.e., AR is maximum at P_{in} approaching zero and P_{out} is maximum at very large P_{in} for which the amplification ratio is one. Thus, the interplay between AR and P_{out} must be understood.

To identify the parameters that determine amplifier performance and to characterize the output of a MOPA configuration, amplifier performance was measured[6] as a function of P_{in}, X_{ib}, flowfield match/mismatch between the oscillator and amplifier, flow rates in the amplifier, the oscillator resonator type (stable or unstable), the time-dependent oscillations of the input beam, and the oscillator used (CL I, 15 cm gain length; or CL II, 30 cm gain length).

Amplifier performance was measured as a function of P_{in} and amplifier flow rates. Table 1 presents data for P_{in}, P_{out}, and AR at the X_{ib} for peak amplification, for both Runs 34 and 36 in the amplifier. Although amplifier performance is not a function of flowfield matching, discussed below, the oscillator flow rate that generated a given P_{in} is included in Table 1 for completeness. The higher amplifier performance occurred at Run 36 flow rates and is plotted as P_{out} vs P_{in} at the X_{ib} for peak amplification (Fig. 5). Figure 5 shows that, at the lowest P_{in}, 4.1 W, the increment $P_{out} - P_{in} = \Delta$ is 13.49 W. Δ increases with P_{in} up to a $P_{in} = 32.2$ W at which point $\Delta = 33.2$ W. As P_{in} continues to increase, Δ remains almost constant.

The reason for this behavior is that only a certain amount of energy can be extracted from the amplifier medium. Once P_{in} is large enough to extract this energy from the flow, an increase in P_{in} still extracts the same amount of energy from the flow; thus, Δ is a constant. In particular, for the CL II gain cell at Run 36 flow rates, the maximum power extracted from the amplifier, Δ, was 33.2 W, whereas the maximum oscillator power was 76 W.[6] This shows that operating the CL II as an amplifier extracts only about 44% of the available energy in the flow.

The CL II oscillator performance[6] at Run 36 flow rates with a 20% reflective outcoupler is 36 W and 76 W with an 80% reflective outcoupler. Figure 5 shows that to obtain a total power of 36 W after the amplifier, about 12 W must be input, and to obtain 76 W after the amplifier, about 40 W must be input. These data show that between one-third and one-half of the device's oscillator output must be input to obtain amplifier output equal to the device's oscillator performance when the oscillator is operated with a 20% and 80% reflective outcoupler, respectively.

Table 1 Output power and amplification ratio as a function of input power at the X_{ib} for peak amplification for Run 34 and Run 36 flow rates at low pressure in the CL II amplifier

Run number				
OSC	AMP	P_{in}, W	P_{out}, W	AR
34	34	4.00	14.12	3.33
36	34	4.60	15.64	3.99
34	34	6.99	23.09	3.30
36	34	6.75	22.49	3.67
34	34	20.45	41.92	2.40
36	34	21.47	42.94	2.19
36	34	33.74	62.88	1.89
35	34	43.96	70.54	1.65
CSS	34*[a]	74.83	98.62	1.33
34	36	4.10	17.59	4.32
36	36	4.96	19.32	4.30
34	36	6.61	25.58	3.86
36	36	6.95	25.30	3.82
36	36	8.31	27.18	3.37
36	36	12.26	36.24	2.91
34	36	20.45	46.01	2.47
36	36	21.47	48.56	2.38
36	36	32.20	65.40	2.17
35	36	42.94	75.66	1.80
CSS	36*[a]	68.12	97.40	1.44

OSC, oscillator; AMP, amplifier; CSS, denotes flow rates with concentric sonic slit He injectors on the oscillator.
[a]High pressure in the amplifier is due to the high flow rates of Run CSS in the oscillator.[6]

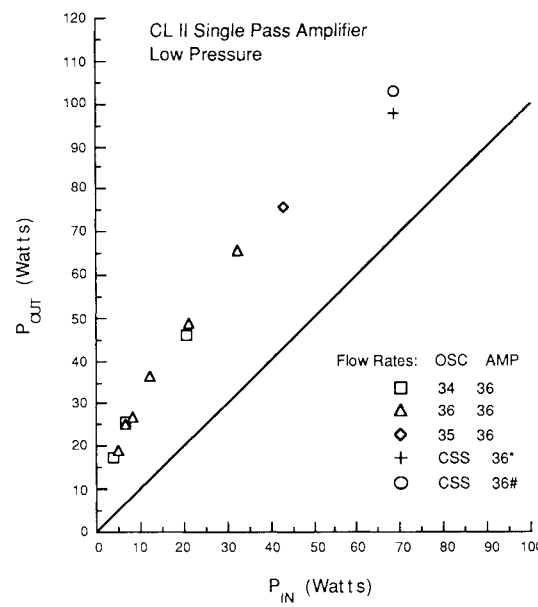

#This data point is the CSS/36* data point after a correction for the high pressure present in the amplifier has been made[6].

Fig. 5 Output power vs input power at the X_{ib} for peak amplification for several oscillator/amplifier flow rate combinations for Run 36 flow rates in the amplifier.

Power spectral distributions (PSDs) before and after the amplifier were obtained for P_{in} of 7.0–75.0 W. Figure 6 is a sample PSD for a P_{in} of 7.0 W. The PSDs show that, at low P_{in}, the distribution of power within the 1→0 and the 2→1 vibrational bands is changed slightly by the amplifier, and in some cases, the amplifier decreases the fraction of power in the 1→0 vibrational band of the output PSD. At high P_{in}, the amplifier has no effect on the output PSD. The reason that

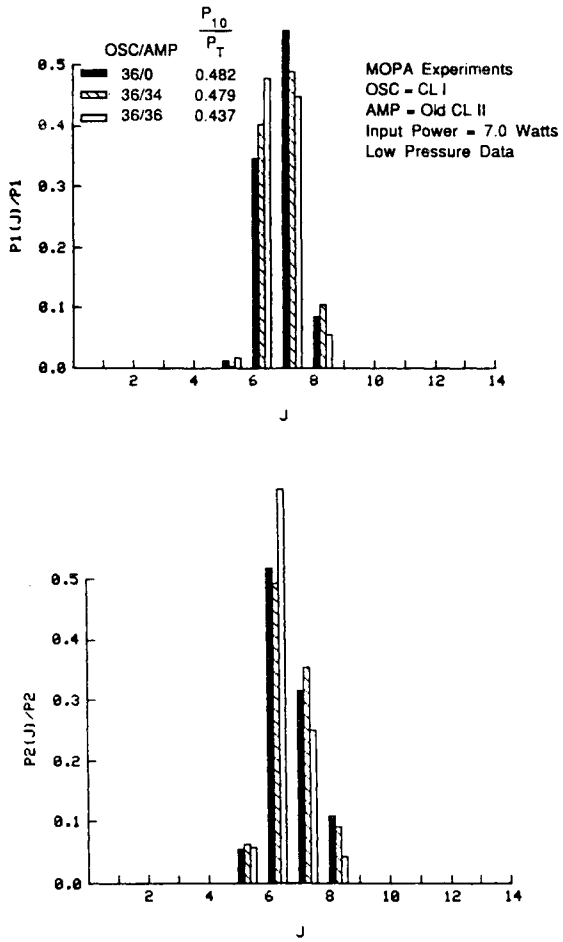

Fig. 6 Power spectral distributions before (36/0) and after (36/34, 36/36) the amplifier at the X_{ib} for peak AR with Run 36 flow rates in the oscillator and Run 34 or Run 36 flow rates in the amplifier at an input power of 7.0 W. The oscillator was the CL I and the amplifier was a CL II.

the amplifier has only a minimal effect on the PSD is the similarity between the input PSD and the zero power gain distribution of the amplifier.[5]

Amplifier performance as a function of P_{in} and flowfield match/mismatch between the oscillator and amplifier was measured for three P_{in} (4.0, 7.0, and 20.0 W) and four different combinations of oscillator/amplifier flow rates. With the same flow rates (run number) in both the oscillator and amplifier, the flowfields are matched. With different flow rates in the oscillator and amplifier, the flowfields are different. This makes the gain, intensity, and spectral distributions mismatched between the two devices. When discussing the flowfield in the oscillator, reference to the intensity distribution of the oscillator is implied. When discussing the flowfield in the amplifier, reference to the zero power gain distribution in the amplifier is implied.

Amplification ratio data were obtained with flow rate combinations 34/34, 34/36, 36/34, and 36/36 in the oscillator/amplifier (OSC/AMP), respectively, at each input power. Figure 7 is a sample of these data at one run combination, OSC/AMP = 36/34, for the three P_{in}. Spectra at the X_{ib} for peak amplification before and after the amplifier were taken for the aforementioned run combinations at the 7.0- and 20.0-W input powers. Figure 6 is a sample PSD for two OSC/AMP run combinations at a P_{in} of 7.0 W.

The most striking results evident from the AR vs X_{ib} data (Fig. 7) are that the amplification ratio is an inverse function of the input power (intensity) and is a sensitive function of the location of the axis of the input beam with respect to the H_2 injectors of the amplifier independent of the match or mismatch of the oscillator/amplifier flowfields.

Comparison of the X_{ib} for peak AR and the width of the gain zone (AR > 1) in the amplifier with the X_{ib} for peak zero power gain and the width of the zero power gain zone measured in the amplifier[5] (Table 2) shows that, for maximum amplification, the peak of the input intensity distribution should be matched to the peak of the zero power gain distribution in the amplifier. The unstable resonator data, discussed in the next section, show that this is true regardless of the resonator used to generate the input beam.

To explore the effect of flowfield match/mismatch in the oscillator/amplifier, Table 3 compares peak ARs as a function of input power for Run 34 and Run 36 flow rates in the amplifier. This comparison shows that the match/mismatch of the oscillator/amplifier flowfields has a second-order effect on amplifier performance, in most cases 10% or less, compared to the effects of X_{ib} and P_{in}. PSDs (Fig. 6), show that the distribution of power within the 1→0 and the 2→1 vibrational bands of the amplifier output PSD is insensitive to oscillator/

Table 2 X_{ib} for peak AR and width of gain zone compared to X_{ib} for peak zero power gain and width of the zero power gain zone for Run 34 and Run 36 flow rates in the amplifier

Amplifier flow rate	X_{ib} for peak AR	Width of gain zone	X_{ib} for peak zero power gain	Width of zero power gain zone
Run 34	1.0–1.5 mm	5.0–5.5 mm	1.0–2.0 mm	4.0–6.0 mm
Run 36	1.0–1.5 mm	4.5–5.0 mm	1.0–1.5 mm	3.5–5.5 mm

Table 3 Peak amplification ratios (ARs) for different OSC/AMP flow rate combinations and input powers

OSC/AMP	Peak amplification ratio (AR)		
	P_{in} = 4.0 W	P_{in} = 7.0 W	P_{in} = 20.0 W
34/34	3.33	3.30	2.40
36/34	3.99	3.67	2.19
34/36	4.32	3.86	2.47
36/36	4.30	3.82	2.38

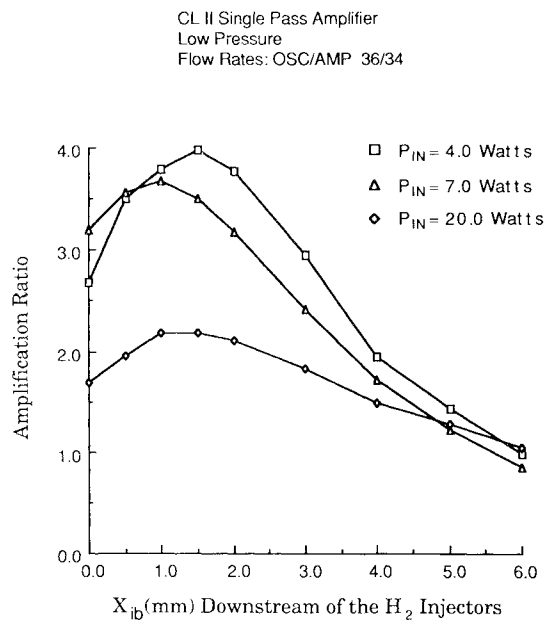

Fig. 7 Amplification ratio as a function of the location of the axis of the input beam with respect to the hydrogen injectors with OSC/AMP = 36/34 flow rates for input powers of 4.0, 7.0, and 20.0 W.

amplifier flowfield match/mismatch. These results demonstrate that losses due to flowfield mismatch are small compared to other effects.

Experiments to determine the effect of the oscillator used (CL I or CL II) showed that amplifier performance is independent of the oscillator used. Experiments to determine the isolation of the oscillator from the amplifier showed that there was no change in the characteristics of the oscillator output (power, power spectral distribution, temporal stability) when the oscillator output beam was injected into the amplifier.

IV. Effect of Resonator on Amplifier Performance

When power is extracted from an oscillator with an unstable resonator, a time-dependent oscillation in the output power may occur on lines whose saturated gain does not fill the unstable resonator. The characteristics of these time-dependent oscillations were studied experimentally and theoretically.[7-10] The effects of the unstable resonator and the temporal variations on amplifier performance are summarized in this section.

A schematic of the layout of the unstable resonator experiments is shown in Fig. 8. A confocal, unstable resonator with magnification 2 and a 1-m mirror separation was used.[8] The amplitude and frequency of the time-dependent oscillations were measured by placing an InAs fast detector at locations 1 and 6. A chopper was always placed in front of the InAs detector to allow measurement of the square wave required to calculate the amplitude modulation of the beam. The outcoupled beam of the unstable resonator (UR) differs from that of the stable resonator (SR). The UR beam has a hole in it. This hole is the result of the variable slit scraper mirror that outcouples the beam in two sections. The section of the beam that is outcoupled by the upstream scraper mirror will be referred to as the upstream beam (UB) and the section of the beam that is outcoupled by the downstream scraper mirror will be referred to as the downstream beam (DB).

Initial experiments consisted of blocking the DB with one of the knife edges (Fig. 8). The UB was then injected into the amplifier using the same technique as the SR amplifier experiments, that is, at $X_{ib} = 0$, the UB was centered on the H_2 injectors. The next experiments injected both the UB and DB sections into the amplifier simultaneously. As in the SR amplifier experiments, the beam sections were passed through the two-lens telescope and injected through the amplifier such that the spatial relationship of the beam with respect to the flowfield was the same in the amplifier and oscillator.

With the DB blocked and the UB injected into the amplifier, amplifier performance for P_{in} of 1.2 and 5.1 W was measured. The P_{in} correspond to scraper mirror slit widths of 4 mm ($N_F = 5.714$) and 2 mm ($N_F = 1.428$), respectively. Thus, the 1.2-W input beam had the 7-ns and 40-ns oscillations present and the 5.1-W input beam had only the 7-ns oscillation present.[8] AR vs X_{ib} data were obtained with Run 34 flow rates in both the oscillator and amplifier at the two input powers. These data are compared with SR amplifier data obtained at a similar P_{in} (4.0 W) (Fig. 9). Figure 9 shows that the UR data are similar to the SR data when the difference in P_{in} is accounted for, i.e., higher P_{in} should have lower ARs and lower P_{in} should have higher ARs. This indicates that amplifier performance is unaffected by the oscillations present in the input beam and amplifier performance is independent of the resonator used to drive the amplifier. Amplifier performance is the same for the UR- and the SR-generated input beams because the input powers were the same and the input power spectral distributions for the UR and SR at Run 34 flow rates contain essentially the same lines. As in the case of the SR beam, maximum amplification occurred when the peak of the input intensity distribution was matched to the peak of the zero power gain distribution in the amplifier.

Amplifier performance as a function of the section of the UR beam used to drive the amplifier was measured. Data were obtained with the UB, DB, and both UB and DB driving the amplifier. The alignment for these experiments used the entire UR beam with the hole in the UR beam aligned with the H_2 injectors of the amplifier at $X_{ib} = 0$. When both the UB and DB were simultaneously injected into the amplifier, they sampled separate regions of the amplifier's gain distribution. To obtain the data when only the UB or DB was injected, the appropriate knife edge (Fig. 8) was used to block the other section of the input beam. This ensured that the alignment of the UB, when injected by itself, was the same as when it was injected with the DB. The same was also true for the DB alignment. Amplifier performance when the entire UR beam was injected was less than when a SR beam was injected at the same input powers and amplifier flow rates.

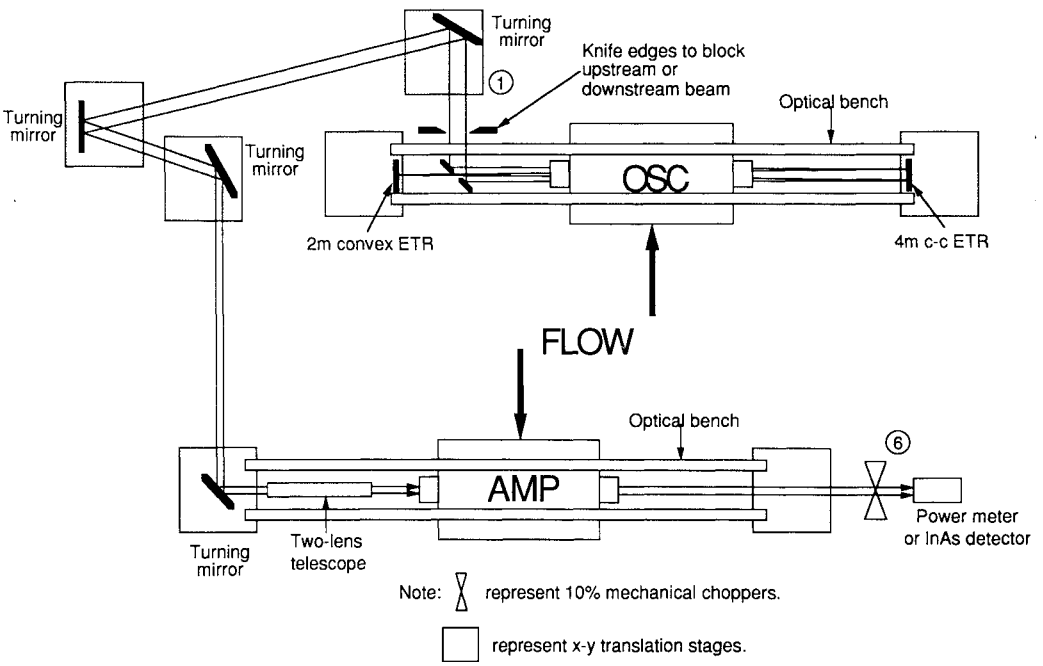

Fig. 8 Schematic of the experimental layout used for unstable resonator MOPA experiments.

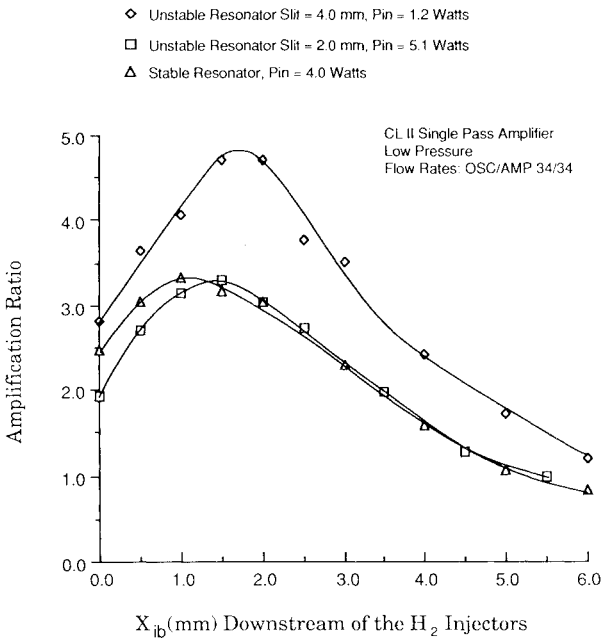

Fig. 9 Amplification ratio as a function of the location of the axis of the input beam with respect to the hydrogen injectors for OSC/AMP = 34/34 flow rates when the input beam is generated by a stable and an unstable resonator.

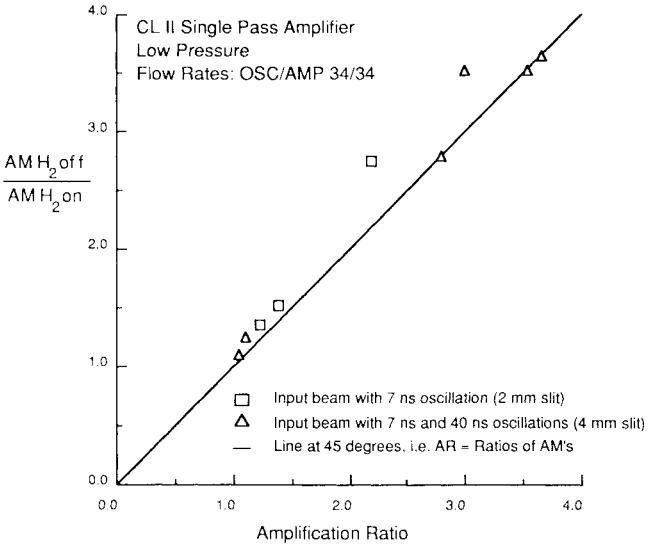

Fig. 10 Ratio of amplitude modulation (AM) before (H_2 off) the amplifier to amplitude modulation after (H_2 on) the amplifier as a function of amplification ratio.

The reduced performance is a result of the hole in the unstable resonator beam that does not allow the intensity distribution of the input beam to match the zero power gain distribution in the amplifier.

The sum of the amplifier output powers when the UB and DB were injected separately was equal to the amplifier output power when both the UB and DB were injected simultaneously. This indicates that amplifier performance at the DB location is independent of the energy removal by the UB injection and vice versa.

When the time-dependent oscillations were present in the input beam, the AR vs X_{ib} was not affected and the amplifier damped the oscillations. The damping of the oscillations is a consequence of the fact that the gain in the amplifier is inversely proportional to the input intensity. Thus, the peaks of the oscillations are amplified less and the valleys are amplified more, resulting in a decrease in the amplitude modulation (AM) of the output beam. The AM decreased by a factor equal to the AR (Fig. 10). The amplifier had no effect on the period (frequency) of the oscillations of the input beam. If the oscillations were not present in the input beam, they did not appear in the output beam of the amplifier, even though the amplifier was capable of producing the time-dependent oscillations if it was run as an oscillator.

V. Concluding Remarks

The most striking results of this study were that the amplification ratio is an inverse function of the input power (intensity) and that, for maximum amplification, the peak of the input intensity distribution should be matched to the peak of the zero power gain distribution in the amplifier. These results were true regardless of the resonator or oscillator used to generate the input beam. The data showed that the match/mismatch of the oscillator/amplifier flowfields has a second-order effect on amplifier performance, in most cases 10% or less, compared to the effects of X_{ib} and power of the input beam. Since amplifier performance is a strong function of input power, to compare amplifier performance when a variable is changed, it is essential that the input power be kept constant.

A somewhat surprising result of the study of P_{out} vs P_{in} at the X_{ib} for peak amplification was that, after a continuous increase, the difference $P_{out} - P_{in}$ remained almost constant over a wide range of input powers. These data showed that between one-third and one-half of the device's oscillator output must be input to obtain amplifier output equal to the device's oscillator performance.

When power is extracted from an oscillator with an unstable resonator, a time-dependent oscillation in the output power may occur on lines whose saturated gain does not fill the unstable resonator. The amplitude modulation of the time-dependent oscillations of the input beam was reduced by a factor that was equal to the amplification ratio of the amplifier. The amplifier had no effect on the period (frequency) of the oscillations of the input beam. If the time-dependent oscillations were not present in the input beam, they did not occur in the output of the amplifier.

When the entire unstable resonator beam was injected into the amplifier, the hole in the beam resulted in reduced amplifier performance compared to stable resonator beam amplifier performance because the unstable resonator beam intensity distribution was not matched to the zero power gain distribution in the amplifier. If the hole in the UR beam could be eliminated (with different optics), the UR beam and SR beam amplifier performance would probably be the same.

Oscillator/amplifier isolation experiments showed that the amplifier had no effect on the performance of the oscillator.

Acknowledgment

This work was supported in part by ONR and W. J. Schafer Associates.

References

[1]Angelbeck, A. W., Boedeker, L. R., Decker, R. O., Foster, M. C., Hasselmark, E., Krascella, N. L., Lynds, L., Mapes, S. N., McMahon, D. G., Meinzer, R. A., Palma, G. E., Sadowski, T. J., Vinje, E. W., Wisner, G. R., and Milan, T. B., "Investigation of Master Oscillator Power Amplifier Systems for Chemical Lasers," AFWL-TR-73-156, United Aircraft Research Laboratories, East Hartford, CT, 1973.

[2]Hoffman, J. M., Patterson, E. L., and Gerber, R. A., "Energy Extraction from a Large-Volume HF Laser Amplifier," *Journal of Applied Physics*, Vol. 50, June 1979, pp. 3861–3866.

[3]Patterson, E. L., Rice, J. K., and Tisone, G. C., "A Master-Oscillator Power Amplifier Experiment for the Determination of the

Gain Coefficient and Saturation Intensity for an Electron-Beam Excited KrF Amplifier," *Applied Physics Letters*, Vol. 36, No. 1, 1980, pp. 188–190.

[4]Bernard, J. M., Chodzko, R. A., and Coffer, J. G., "Master Oscillator with Power Amplifiers: Performance of a Two-Element CW HF Phased-Laser Array," SD-TR-89-40, The Aerospace Corp., El Segundo, CA 90245, June 15, 1989.

[5]Sentman, L. H., Theodoropoulos, P., Waldo, R., Nguyen, T., and Snipes, R., "An Experimental Study of cw HF Chemical Laser Amplifier Performance and Zero Power Gain," AAE TR 87-6, UILU Eng. 87-0506, Aeronautical and Astronautical Engineering Dept., University of Illinois, Urbana, IL, Aug. 1987.

[6]Sentman, L. H., Waldo, R., Nguyen, T., and Theodoropoulos, P., "cw HF Chemical Laser Oscillator/Amplifier Performance in a MOPA Configuration," TR 88-7, UILU Eng. 88-0507, Aeronautical and Astronautical Engineering Dept., University of Illinois, Urbana, IL, July 1988.

[7]Sentman, L. H., "Chemical Laser Power Spectral Performance: A Coupled Fluid Dynamic, Kinetic and Physical Optics Model," *Applied Optics*, Vol. 17, 1978, pp. 2244–2249.

[8]Sentman, L. H., Nayfeh, M. H., Townsend, S., King, K., Tsioulos, G., and Bichanich, J., "Time-Dependent Oscillations in a cw Chemical Laser Unstable Resonator," *Applied Optics*, Vol. 24, No. 21, 1985, pp. 3598–3609.

[9]Sentman, L. H., Carroll, D. L., Theodoropoulos, P., and Gumus, A., "Scale Effects in a cw HF Chemical Laser," AAE TR 86-5, UILU Eng. 86-0505, Aeronautical and Astronautical Engineering Dept., University of Illinois, Urbana, IL, Sept. 1986.

[10]Sentman, L. H., and Gilmore, J. O., "Computer Simulation of cw HF Chemical Laser Unstable Resonator Performance," AAE TR 87-5, UILU Eng. 87-0505, Aeronautical and Astronautical Engineering Dept., University of Illinois, Urbana, IL, Aug. 1987.

Recommended Reading from the AIAA Progress in Astronautics and Aeronautics Series . . . AIAA

Dynamics of Flames and Reactive Systems and Dynamics of Shock Waves, Explosions, and Detonations

J. R. Bowen, N. Manson, A. K. Oppenheim, and R. I. Soloukhin, editors

The dynamics of explosions is concerned principally with the interrelationship between the rate processes of energy deposition in a compressible medium and its concurrent nonsteady flow as it occurs typically in explosion phenomena. Dynamics of reactive systems is a broader term referring to the processes of coupling between the dynamics of fluid flow and molecular transformations in reactive media occurring in any combustion system. *Dynamics of Flames and Reactive Systems* covers premixed flames, diffusion flames, turbulent combustion, constant volume combustion, spray combustion nonequilibrium flows, and combustion diagnostics. *Dynamics of Shock Waves, Explosions and Detonations* covers detonations in gaseous mixtures, detonations in two-phase systems, condensed explosives, explosions and interactions.

Dynamics of Flames and Reactive Systems
1985 766 pp. illus., Hardback
ISBN 0-915928-92-2
AIAA Members $59.95
Nonmembers $92.95
Order Number V-95

Dynamics of Shock Waves, Explosions and Detonations
1985 595 pp., illus. Hardback
ISBN 0-915928-91-4
AIAA Members $54.95
Nonmembers $86.95
Order Number V-94

***TO ORDER:* Write, Phone, or FAX:** American Institute of Aeronautics and Astronautics c/o Publications Customer Service, 9 Jay Gould Ct., P.O. Box 753, Waldorf, MD 20604 Phone: 301/645-5643 or 1-800/682-AIAA, Dept. 415 ■ FAX: 301/843-0159

Sales Tax: CA residents, 8.25%; DC, 6%. For shipping and handling add $4.75 for 1–4 books (call for rates for higher quanties). Orders under $50.00 must be prepaid. Foreign orders must be prepaid. Please allow 4 weeks for delivery. Prices are subject to change without notice. Returns will be accepted within 15 days.